

Registration-Based Motion Correction in Time-Series Studies of Bone Microarchitecture and Mechanics

Ning Zhang¹, Jeremy F Magland¹, Chamith S Rajapakse¹, Hee Kwon Song¹, and Felix W Wehrli¹
¹University of Pennsylvania, Philadelphia, PA, United States

Introduction: Subject motion in MR imaging causes image artifacts such as ghosting and blurring, thereby reducing the reliability of image-based quantitative analysis and the data's diagnostic usefulness¹. Problems from subject motion are exacerbated when imaging trabecular bone (TB) due to the high resolution required to accurately retrieve bone 3D micro-structure and the associated relatively long scan time. Although navigator-based² or autofocusing³ motion correction techniques alleviate motion artifacts, correction of both translational and rotational motion is problematic for the former in TB imaging and the image sharpness metrics used in the latter are often susceptible to noise. Here, we present a registration-based approach for automatically rigid-body retrospective motion correction. In-vivo experiments were conducted on the distal radius, an anatomical site where rotational motion occurs more frequently, to evaluate the technique's performance and effectiveness on improving serial reproducibility.

Methods: The new technique involves three steps. First, we assume that one image in the time series of acquired images is less motion corrupted than the others. This image is used as the "reference" to correct the other motion-degraded images. A pattern-based registration⁴ is performed to resample the reference to each of the corrupted images. Next, motion-induced displacements in the corrupted images are corrected based on the reference. As in traditional autofocusing³ k-space data of the corrupted image is divided into small segments, which are corrected one at a time (starting from the center of k-space and moving outward) by applying a series of trial rotations and translations (the remaining segments being fixed). The objective here is to maximize the cross-correlation between the corrupted and reference images within a region of interest (typically TB region), as opposed to optimizing an image sharpness metric for individual scans separately in traditional autofocusing³. This segment-based optimization is performed in an iterative manner, i.e., when all segments with a given size have been optimized, a new iteration starts with a reduced segment size. Lastly, if there are more than two time points in the series, the third step is to resample the corrupted images after correction back to their reference for subsequent quantitative analysis (see **Figure 1** for an illustration of the procedure).

The technique's performance was evaluated based on measurement of serial reproducibility of structural and mechanical parameters in the distal radius of 12 women (ages 50-75). All in-vivo μ MR images were acquired as part of a previous study⁵ at three time points using a 3D fast large angle spin echo (FLASE) sequence⁶ with a voxel size of $137 \times 137 \times 410 \mu\text{m}^3$ at 1.5T field strength. Reconstructed images were motion corrected using navigator-based correction, autofocusing and registration-based correction (translation only as well as rotation/translation combined) separately for comparison.

Structural parameters, including BV/TV, surface to curve ratio (S/C) and erosion index (EI) were calculated via digital topological analysis (DTA)⁷ based virtual bone biopsy (VBB) processing⁸. Trabecular thickness (Tb.Th) was calculated using fuzzy distance transform⁹ and trabecular number (Tb.N) derived as in⁵. Mechanical parameters, including axial stiffness, yield strain/stress, ultimate strain/stress, modulus of resilience and toughness, were calculated using linear and nonlinear micro-finite-element (μ FE) analysis^{10,11} under simulated compressive loading in the axial direction.

Coefficients of variation (CV) and intra-class correlation coefficient (ICC) were calculated as measures of reproducibility.

Results and Discussion: The percent changes of NGS, a measure of image sharpness, relative to no correction were 0.07%, 1.09%, 3.73%, 3.90% and 3.92%, respectively, for navigator-based, autofocusing, translation only as well as rotation/translation combined registration-based correction (**Figure 2**). In terms of reproducibility, the average CV over all parameters (structural and mechanical) decreased from 5.6% to 4.9%, 4.1%, 3.7% and 3.5%, respectively for the navigator-based technique, autofocusing, the registration-based technique (without and with rotation correction). Similarly, average ICC increased from 0.948 to 0.959, 0.969, 0.974 and 0.978, respectively (**Figure 3**).

Conclusion: These results suggest that rigid-body motion artifacts in 3D high-resolution trabecular bone imaging can be retrospectively corrected by using a relatively motion-free image in the time series as reference. The registration-based motion correction approach presented here has been shown to correct for intra-scan motions thereby improving the serial reproducibility of image-derived estimates in longitudinal studies.

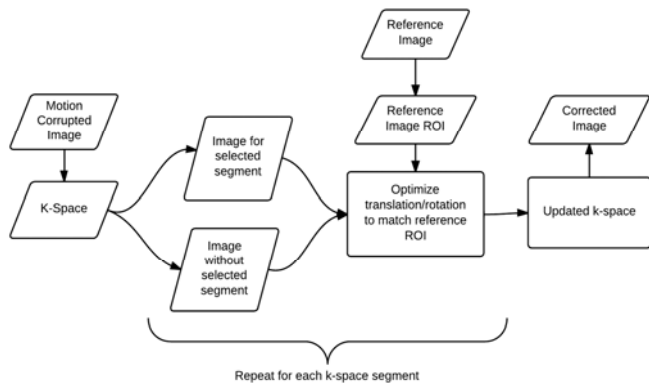


Figure 1. Motion correction processing pipeline: k-space is divided into segments each of which was corrected sequentially by applying trial displacements to maximize the cross-correlation with the reference within ROI (the TB region).

References: [1] Gomberg, Bone, 2004; [2] Song, MRM, 1999; [3] Lin, JMRI, 2007; [4] Magland, JMRI, 2009; [5] Lam, Bone, 2011; [6] Magland, MRM, 2009; [7] Saha, Int J Imaging Syst Technol, 2000; [8] Magland, Acad Radiol, 2008; [9] Saha, IEEE Trans Med Imaging, 2004; [10] Magland, PLoS ONE, 2012; [11] Zhang, Med. Phys., 2013.

Acknowledgement: NIH grants R01 AR55647 and R01 AR054439.

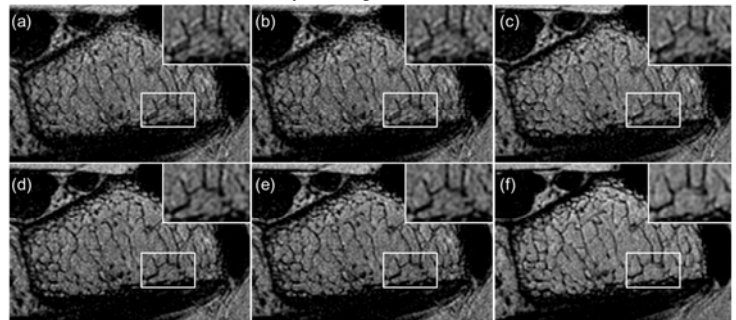


Figure 2. Distal radius images along with expanded region (inset): (a) Motion-corrupted image, (b) navigator-based technique corrected image, (c) AF corrected image, (d) registration-based technique corrected image (without correction for rotational motion), (e) registration-based technique corrected image (with correction for rotation), and (f) the reference image of the distal radius from a subject.

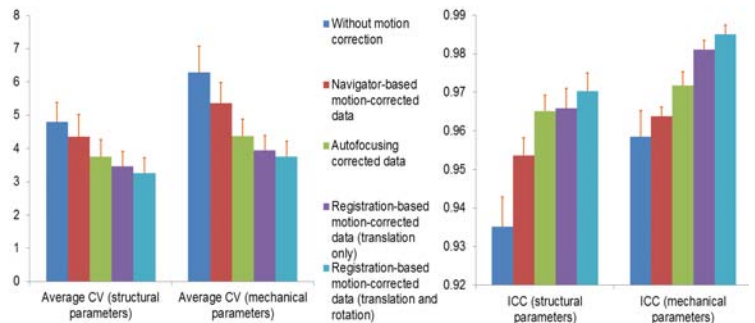


Figure 3. Comparisons of (a) average CV and (b) ICC (averaged over structural and mechanical parameters) obtained without and with applying various motion correction techniques.